Available online at www.sciencedirect.com
ScienceDirect
Bioorganic & Medicinal Chemistry 14 (2006) 7862–7874
Bioorganic & Medicinal Chemistry

Delivery of 2-5A cargo into living cells using the Tat cell penetrating peptide: 2-5A-tat

Longhu Zhou,[a] Chandar S. Thakur,[b] Ross J. Molinaro,[b] Jayashree M. Paranjape,[b] Rieuwert Hoppes,[c] Kuan-Teh Jeang,[c] Robert H. Silverman[b] and Paul F. Torrence[a,d,*]

[a]*Department of Chemistry and Biochemistry, Northern Arizona University, Flagstaff, AZ 86011-5698, USA*
[b]*Department of Cancer Biology, Lerner Research Institute, Cleveland Clinic, 9500 Euclid Avenue, Cleveland, OH 44195, USA*
[c]*Molecular Virology Section, Laboratory of Molecular Microbiology, National Institute of Allergy and Infectious Diseases, National Institutes of Health, Bethesda, MD 20892, USA*
[d]*Department of Chemistry, Cleveland State University, Cleveland, OH 44115, USA*

Received 8 June 2006; accepted 27 July 2006

Abstract—2′,5′-Oligoadenylate tetramer (2-5A) has been chemically conjugated to short HIV-1 Tat peptides to provide **2-5A-tat** chimeras. Two different convergent synthetic approaches have been employed to provide such **2-5A-tat** bioconjugates. One involved generation of a bioconjugate through reaction of a cysteine terminated Tat peptide with a α-chloroacetyl derivative of 2-5A. The second synthetic strategy was based upon a cycloaddition reaction of an azide derivative of 2-5A with a Tat peptide bearing an alkyne function. Either bioconjugate of **2-5A-tat** was able to activate human RNase L. The union of 2-5A and Tat peptide provided an RNase L-active chimeric nucleopeptide with the ability to be taken up by cells by virtue of the Tat peptide and to activate RNase L in *intact cells*. This strategy provides a valuable vehicle for the entry of the charged 2-5A molecule into cells and may provide a means for targeted destruction of HIV RNA in vivo.

1. Introduction

Interferon stimulated genes encode proteins which mediate all of the biological effects of interferons.[1,2] One set of interferon stimulated genes comprise the 2-5A* synthetase enzymes which produce a short oligonucleotide called 2-5A (**1**, Fig. 1). This molecule plays a pivotal role in the 2-5A system. Exposure of a cell to interferon induces enhanced levels of 2-5A synthetase. Then dsRNA, formed as an intermediate in viral replication, activates the synthetase to generate 2-5A from ATP. 2-5A provides an unambiguous signal to initiate RNA decay in mammalian cells through activation of latent 2-5A-dependent RNase L that degrades mRNA and rRNA, thereby inhibiting translation. RNase L is thus converted from a silent to an active form by binding with 2-5A.

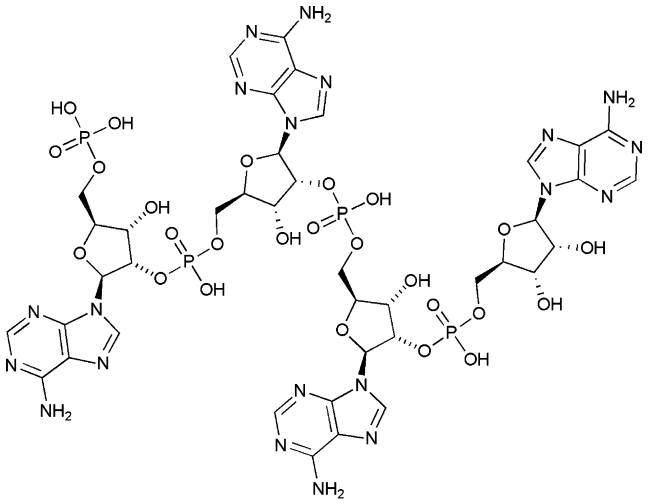

1

Figure 1. 2-5A tetramer, p5′A2′p5′A2′p5′A2′p5′A.

Abbreviations: 2-5A refers to a 2′, 5′-phosphodiester linker oligoadenylate of varying chain length of general formula $(p5'A2'p)_n5'A$; dsRNA, double-stranded ribonucleic acids; RNase L, ribonuclease L; Tat, full-length peptide; tat, generic for truncated versions of Tat; **2-5A-tat**, generic for conjugates of 2-5A with tat peptides.

Keywords: Ribonuclease L; Interferon; Cycloaddition; Sulfhydryl alkylation; RNA; 2′,5′-Oligoadenylate.

* Corresponding author. Tel.: +928 523 0298; fax: +928 523 8111; e-mail: Paul.Torrence@nau.edu

0968-0896/$ - see front matter © 2006 Elsevier Ltd. All rights reserved.
doi:10.1016/j.bmc.2006.07.058

A major barrier to the fruitful application of 2-5A to therapeutic situations has been the difficulty of delivery to cells. Adequate uptake of the 2-5A oligonucleotide requires treatments with hypotonic salts, calcium co-precipitates, or cationic lipids, none of which are suitable for therapeutic applications.[1] This paper reports a solution to this latter uptake dilemma and may provide an approach for targeting of RNase L to HIV RNA in cultured cells and potentially in vivo. This strategy is based upon the molecular biology of HIV replication.

Interaction of the TAT protein with HIV RNA. For over a decade, it has been known that the HIV Tat regulatory protein stimulates transcription of the HIV RNA by binding to the transactivation-responsive region (TAR) located in the 5′-terminus of the HIV RNA, just downstream of the transcriptional initiation site in the HIV genome. Although the Tat protein is 101 amino acids in length, the C-terminal domain, which contains a nine amino acid arginine-rich region, binds to the TAR RNA with the avidity of the full-length Tat.[3] Additional studies have shown that nonapeptides (such as but not limited to Tat amino acids 49–57, RKKRRQRRR) can bind to TAR RNA with affinity approximating the complete Tat protein.[4] The critical role played by the Tat regulatory protein in HIV replication has made it an attractive target for therapeutic interference in HIV/AIDS.[5–21] since interference with the Tat–TAR interaction leads to inhibition of HIV replication.

The Tat protein and the truncated constituent arginine-rich peptide GRKKRRQRRRPPQ, when fused to bioactive peptides or proteins, are able to deliver these molecules into intact cells. These so-called membrane translocation signal (MTS) or cell-penetrating peptides also effect internalization of peptide nucleic acids (PNAs), plasmid DNA, antisense oligonucleotides, paramagnetic cations, and superparamagnetic iron oxide particles. Embedded in the MTS motif of Tat protein is the TAR recognition sequence, **RKKRRQRRR**. The Tat activation domain, which promotes HIV replication and angiogenesis, occurs at Tat residues 21–40, outside the cell-penetrating peptide sequence.

Herein we describe the syntheses of two different **2-5A-tat** peptide conjugates that can be transported into intact cells, activate RNase L, and effect the degradation of cellular RNA.

2. Results

2.1. Synthesis of 2-5A-tat bioconjugates

Two different approaches were employed to join 2-5A tetramer to Tat peptide. First, a chemoselective ligation reaction was used; namely, 1,3-dipolar cycloaddition employing cuprous ion catalyst. This methodology has been widely applied.[22–27] The Cu(I)-catalyzed reaction of terminal alkynes with azides has many advantages including very mild reaction conditions, high yields, high chemoselectivity, and exclusive regioselectivity. To apply it in the present circumstances, a model reaction first was studied. AMP (**2**) was periodate oxidized to the dialdehyde which was reacted with 3-azidopropanamine to yield the corresponding Schiff's base. This was reduced by sodium cyanoborohydride directly without isolation. The product *N*-azidopropylmorpholine (**3**) was obtained in 82% yield after HPLC purification, and its structure was corroborated by proton NMR, phosphorus NMR, and high-resolution mass spectrometry.

To generate the corresponding modification to 2-5A, similar reaction conditions were employed to provide the 2-5A–propyl azide adduct (**4**) from **1** in 45% yield after HPLC purification. Structure corroboration was by MALDI-TOF mass spectrometry: (*m*/*z*, calcd for $C_{43}H_{56}N_{24}O_{23}P_4$: 1400.9; found 1401). The 1,3-dipolar cycloaddition reaction of azido compounds with *N*-hexenyl-modified tat peptide **5** was carried out smoothly in the presence of $CuSO_4$ (1 equiv) and sodium ascorbate (2 equiv) at room temperature in water for 24 h. For the reaction with azido-modified AMP (**3**), the tat adduct (**6**) was obtained (after purification) in 60% yield. The product's structure (**6**) was confirmed by MALDI-TOF mass spectrometry: (*m*/*z*, calcd for $C_{83}H_{152}N_{45}O_{20}P$: 2131; found 2131). The reaction between the azido-modified 2-5A tetramer **4** and tat peptide **5** was carried out under similar conditions. The product **2-5A-tat** (**7**) was corroborated by MALDI-TOF mass spectrometry: (*m*/*z*, calcd for $C_{113}H_{188}N_{60}O_{38}P_4$: 3118; found 3118) (see Fig. 2).

To obtain a **2-5A-tat** conjugate by an independent alternate route, the well-established nucleophilic attack of a cysteine sulfhydryl on a chloroacetyl α-carbon was employed (Fig. 3). Thus, tat peptide was elongated by a cysteine group at the amino-terminus to provide compound **14**. To provide a 2-5A derivative with a reactive chloroacetyl group, a model reaction of AMP with cysteine-functionalized Tat peptide was investigated. AMP first was periodate-oxidized to the dialdehyde which was then reacted with *p*-[(α-chloroacetyl)amino]benzylamine (**11**). The latter was prepared in two steps from *tert*-Boc protected *p*-amino-α-aminotoluene (**8**) and α-chloroacetyl chloride (**9**). The corresponding Schiff's base intermediate from **11** and periodate-oxidized AMP was reduced in situ with sodium cyanoborohydride, $Na(CN)BH_3$. After HPLC purification, this product (**12**) was obtained in a yield of 85%. Its structure was corroborated by proton and carbon NMR and by electrospray mass spectrometry. These successful reaction conditions were then applied to 2-5A tetramer (**1**) to provide the desired 2-5A-chloroacetyl conjugate (**13**) that, after HPLC purification, gave an experimental high resolution mass of 1499.443, in excellent agreement with the predicted mass of 1499.279. Reaction of the chloroacetyl AMP (**12**) and 2-5A derivatives (**13**) with the cys-modified tat peptide was accomplished under oxygen-free conditions to yield both the AMP-tat conjugate (**15**) and the **2-5A-tat** conjugate (**16**). The synthesis of a fluorescently labeled version of conjugate **16** was achieved using essentially the same technique by starting with a custom synthesized peptide Cys-Gly-Gly-Arg-Lys-Lys-Arg-Arg-Gln-Arg-Arg-Arg-fluorescein. The product's structure (Fig. 4, compound **17**) was confirmed by MALDI-TOF.

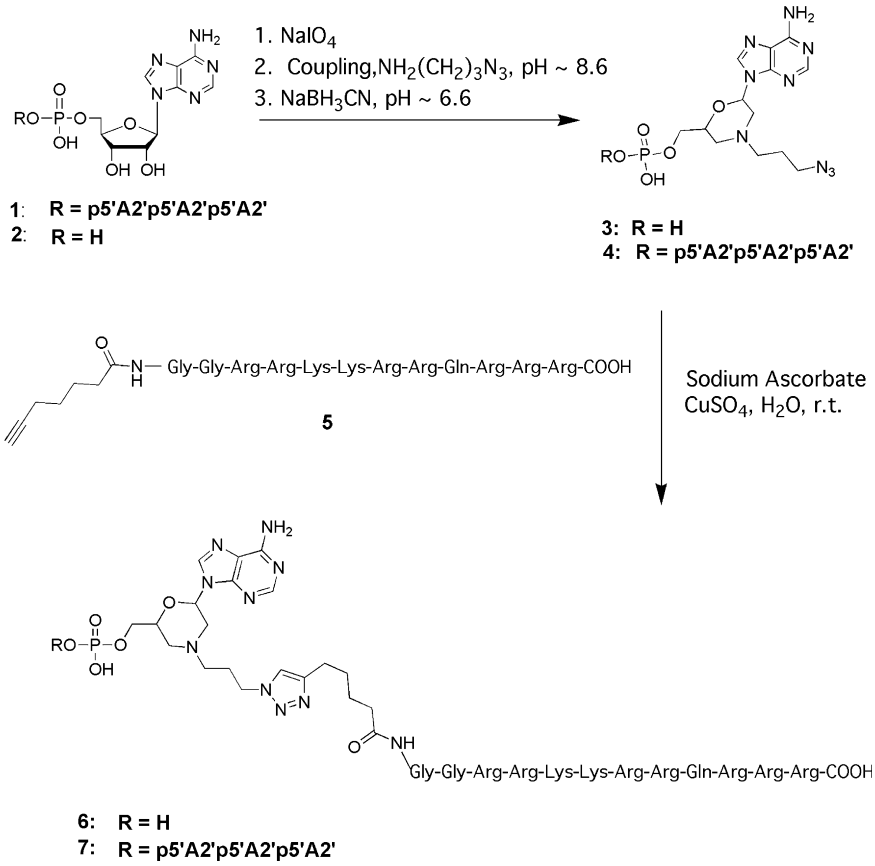

Figure 2. Synthesis of an AMP-tat and a **2-5A-tat** conjugate through generation of a azide-functionalized AMP or 2-5A derivative followed by their respective conjugations to an alkyne-functionalized tat peptide using Cu(I)-catalyzed 1,3-dipolar cycloaddition.

2.2. Activation of homogeneous human RNase L by 2-5A-tat peptide conjugates

The ability of the 2-5A-tat peptide conjugates (**7** and **16**) to activate RNase L was determined by a fluorescence resonance energy transfer (FRET) method.[28] This assay employed recombinant human RNase L produced in insect cells from a baculovirus vector and purified to homogeneity by fast protein liquid chromatography (FPLC).[29] The cleavable substrate was composed of a 36 nucleotide synthetic oligoribonucleotide sequence derived from respiratory syncytial virus with the fluorophore, FAM, at the 5′-terminus and black hole quencher-1 (BHQ-1), at the 3′-terminus (synthesized at Integrated DNA Technologies). The RNA sequence contains several cleavage sites for RNase L (UU or UA). This RNA substrate does not provide a putative target sequence for conjugates **7** or **16**, but is used in this context to evaluate the relative ability of these conjugates to activate human RNase L in comparison to the unmodified activator, 2-5A tetramer itself. Relative fluorescence as a monitor of RNase L enzymatic activity is plotted versus concentration of either pure 2-5A tetramer as a standard, or against the concentration of the respective **2-5A-tat** peptide conjugates **7** or **16** (Fig. 5). Increasing fluorescence corresponds to RNA cleavage as the quencher moiety is released as one fragment of the RNA chain and cannot quench the fluorophore at the other end of the parent chain. RNA cleavage experiments were carried out using several times of incubation with enzyme and activator (Table 1). Figure 5 displays the results of the experiment in which the incubation time was 120 min. First, it is clear from Table 1 that the results at different times of incubation did not vary significantly except for the somewhat higher values obtained at 30 min. Comparison among the different conjugates and 2-5A was based upon an average of the four time determinations (column labeled 'Relative' in Table 1). Second, from Table 1 and Figure 4, it is clear that the **2-5A-tat** peptide chimeras **7** and **16** were able to activate RNase L albeit with less potency than parent 2-5A tetramer itself. Thus, the conjugate (**16**) with the thioether linkage bond displayed an average EC_{50} of 110 nM with the standard 2-5A tetramer (**1**) showing an average EC_{50} of 2.5 nM. The conjugate (**7**) with the triazole ring linkage moiety displayed an average EC_{50} of 300 nM. Thus, the thioether linkage-based conjugate (**16**) was 44 times less effective as an RNase L activator compared to parent 2-5A (**1**). The **2-5A-tat** peptide conjugate **7** was 120-fold less active than parent 2-5A (**1**) and threefold less active than conjugate **16**. When the simple AMP-Tat peptide adducts (compounds **6** and **15**) were evaluated in this RNA cleavage assay, they were totally devoid of activity even at 300 nM, the highest concentration tested (data not shown).

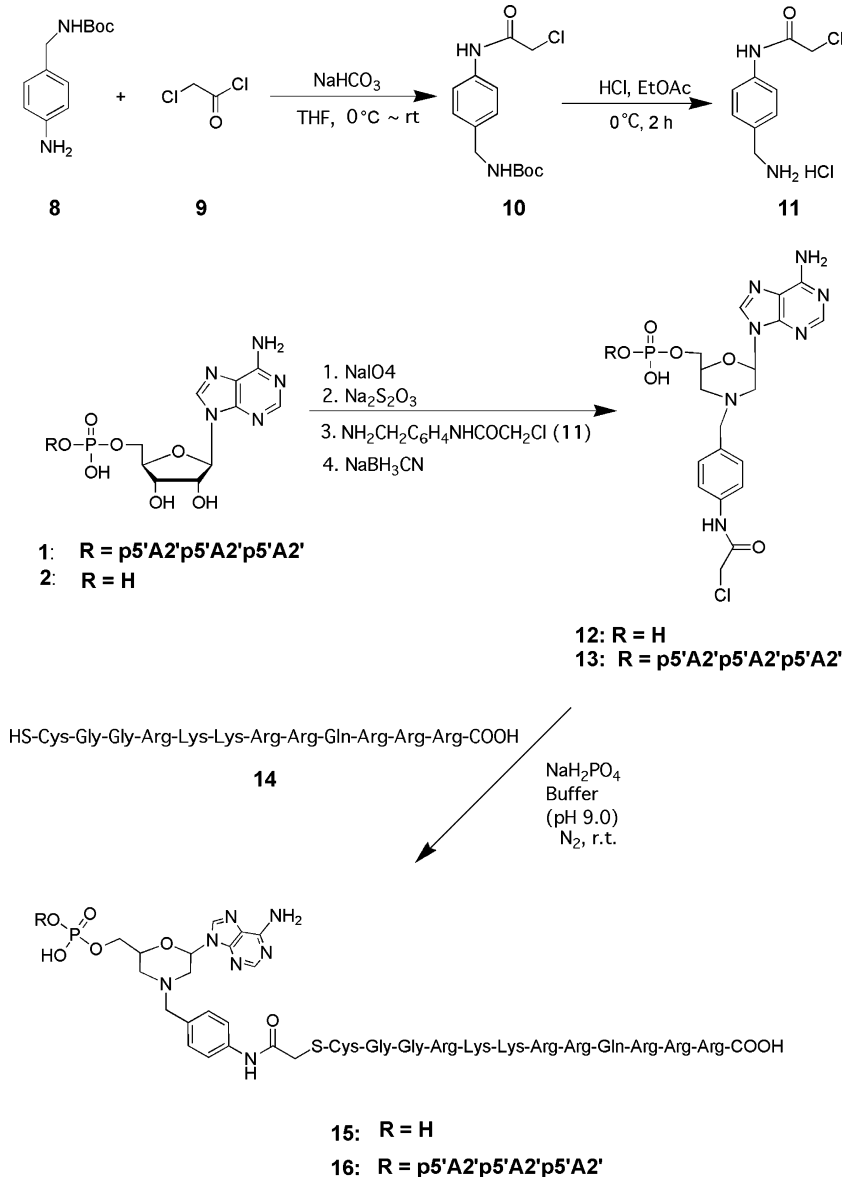

Figure 3. Synthesis of **2-5A-tat** peptide via sulfhydryl-chloroacetyl ligation scheme.

2.3. Uptake of fluorescently labeled 2-5A-tat peptide conjugate by intact cells (Fig. 6)

We first monitored by confocal microscopy to confirm that both fluorescent-tat and fluorescent **2-5A-tat** (Compound **17**) entered cells. Figure 6 provides visual confirmation that indeed both molecules are taken into cells progressively over time. Both fluorescent-Tat and fluorescent **2-5A-tat** (compound **17**) were applied to the cells at a final concentration of 1 μM and images obtained at the indicated times. Images of cellular uptake of compounds were acquired with a Zeiss LSM410 laser scanning confocal microscope equipped with a mixed-gas laser (488-, 568-, and 647-nm excitation lines) in sequential scans and then analyzed with Microcosm Renaissance 410 software. Overlays of the acquired images with corresponding differential interference contrast (DIC) microscopy were generated using Adobe Photoshop CS software.

In Figure 6, panel A shows that fluorescent-tat is surrounding the cells but is not yet taken up. In (B) fluorescent-tat has entered the cytoplasm and a slight accumulation in the nucleus is observed (1 h). In panel (C), after 2 h, fluorescent-tat appears to be most concentrated in the nucleolus and can also still be found in the cytoplasm and nucleus. In panel (D), fluorescent **2-5A-tat** (compound **17**) readily entered the cells and is observed in the cytoplasm, nucleus, and nucleolus. Also, it surrounds the cells in a similar manner as fluorescent-tat at the 10 min timepoint. In panel (E), After one hour, the highest concentration of fluorescent **2-5A-tat** is in the nucleolus, the lowest concentration is seen in the cytoplasm. The cells start to round up at this stage. In panel (F), after two hours, the cells are mostly rounded up, fluorescent **2-5A-tat** concentration in the cytoplasm has dropped and the compound is now clearly most concentrated in the nucleolus. The rounding up of cells seen for compound **17** may be related to the use

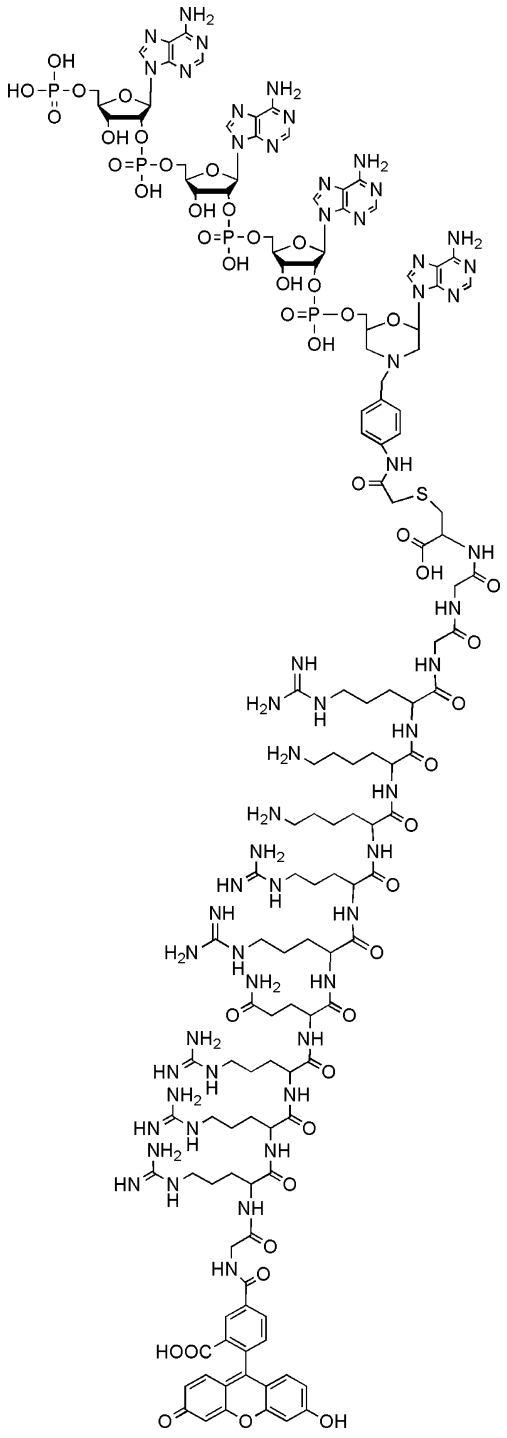

Figure 4. Structure of fluorescent **2-5A-tat**, compound **17**.

of 1 μM concentration of this RNase L activator since even 250 μM 2-5A-tat was able to effect rRNA degradation (vide infra Fig. 7).

2.4. Activation of RNase L in intact cells by 2-5A-tat peptide conjugate

To determine the ability of the **2-5A-tat** conjugate, compound **16**, to both enter cells and activate intracellular RNase L, a HeLa cell line that overexpressed RNase L was employed (Section 5). RNase L is known to cleave

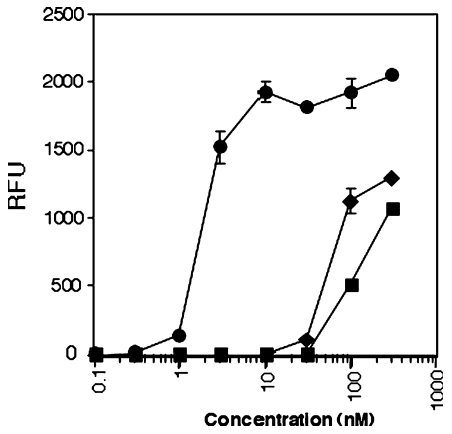

Figure 5. 2-5A-tat fusion molecules activate recombinant RNase L in vitro. Tetrameric 2-5A (circles), and **2-5A-tat** peptide compounds **7** and **16**, (square and diamond symbols, respectively) were incubated at 20 °C for 120 min with purified recombinant RNase L in the presence of a cleavable FRET RNA probe (Section 5). The relative fluorescence units (RFU) (abscissa), a measure of RNase L activity, is plotted as function of compound concentration (ordinate). Error bars represent standard deviations.

rRNA at unique sites in intact ribosomes.[30] Therefore, the endpoint for activation of RNase L in these experiments was rRNA cleavage. All treatments were for 6 h and were performed in duplicate. To provide an appropriate control, 2-5A tetramer (**1**) at a concentration of 5 μM was introduced into cells using the commercial product FuGene 6 (Roche Diagnostics), a multi-component lipid-based (non-liposomal) transfection reagent. On the other hand, the **2-5A-tat** peptide conjugate **16** was simply added to the cells *in the absence of FuGene or any other uptake enhancer*. As is apparent from Figure 7, 2-5A transfection resulted in the characteristic cleavages of 28S and 18S (lanes 5 and 6). No such rRNA cleavage products were visible in the RNA isolated from untreated or FuGene-treated cells. The same distinct and characteristic rRNA cleavage products obtained by 2-5A transfection also were apparent in the RNA isolated from cells treated with **2-5A-tat** peptide conjugate **16** at 250 and 500 nM concentrations (compare lanes 5 and 6 with lanes 9–12). Thus, conjugate **16**, when applied *alone* to these HeLa cells, was able to enter the cells and then effect activation of RNase L leading to rRNA degradation. The reduced level of rRNA cleavage obtained with compound **16** as compared to 2-5A could be due to the lower concentrations of compound **16** that were used and to a reduced ability of this molecule to activate RNase L (Fig. 5). The relative inactivity of compound **16** for cleaving rRNA is actually an advantage in that it could provide a therapeutic window to treat HIV infections with minimal toxicity (Section 3).

3. Discussion

Through the use of two very different conjugation chemistries, 2-5A tetramer has been ligated to Tat peptide. One ligation chemistry involved an S_N2 reaction of the terminal cys of a modified Tat peptide with a 2-5A derivative modified with an α-chloroacetyl group. The second

Table 1. RNase L activation at different times of incubation

Compound	EC_{50}[a] (nM)					
	At 30 min	At 60 min	At 90 min	At 120 min	Average[b]	Relative[c]
2-5A (**1**)	3	2.7	2.2	2.1	2.5	1
16	200	80	80	90	110	44
7	350	300	300	280	300	120

[a] EC_{50}, concentration (nM) of compound that was required to activate RNase L such that 50% of RNA substrate was degraded as evidenced by change in fluorescence.

[b] Average EC_{50}, average of all 4 determinations at different times.

[c] Relative EC_{50}, ratio of EC_{50}s of two activators where the potency of 2-5A tetramer is set arbitrarily to unity: EC_{50} (conjugate)/EC_{50} (2-5A). Thus, relative EC_{50} is a measure of how much more conjugate is required to effect a 50% degradation of RNA as compared to 2-5A itself.

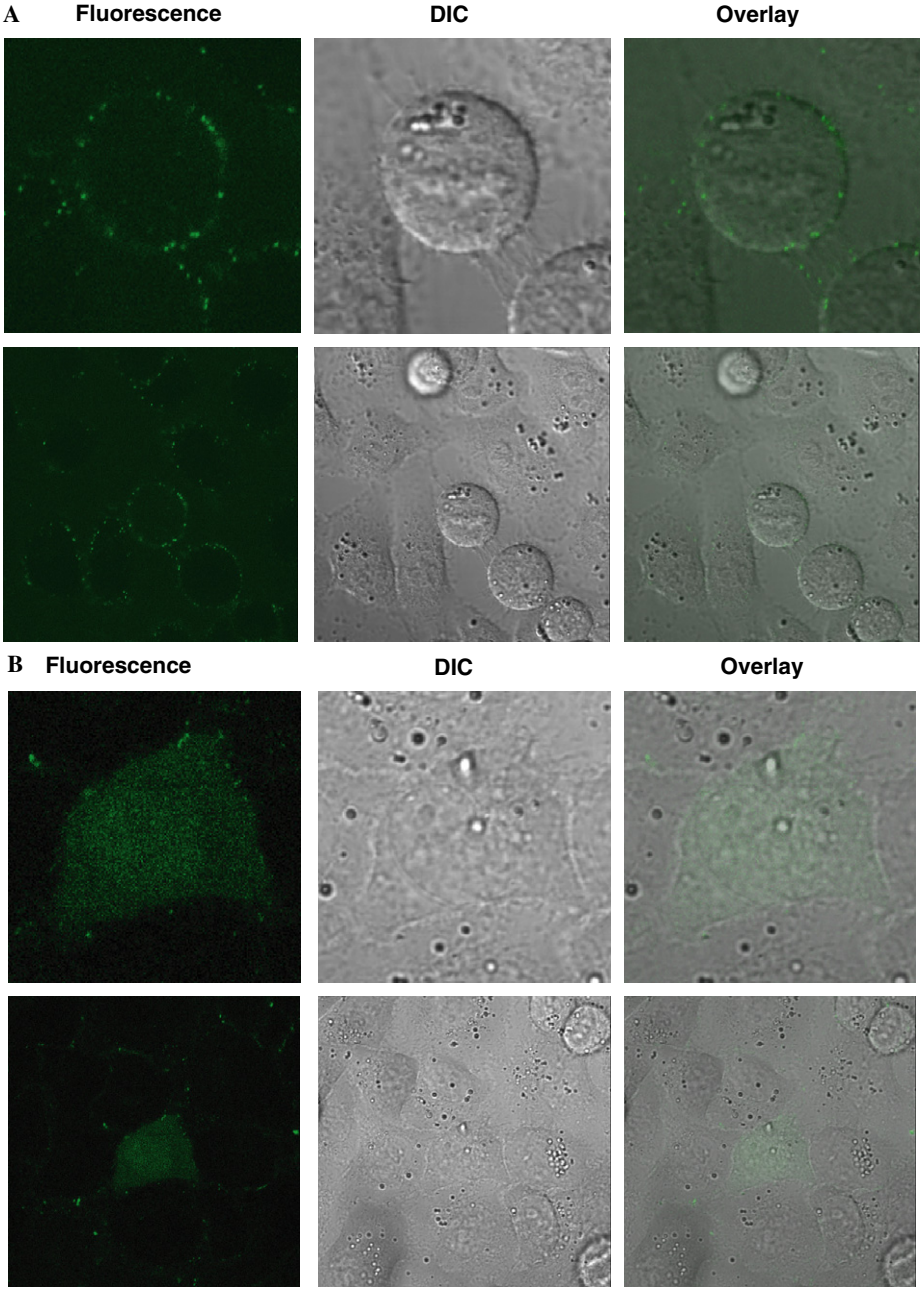

Figure 6. Proof that both **2-5A-tat** and tat can be taken up into cells. Figure 6 monitors uptake over time from 10 mim to 2 h. Apparent is first the attachment to the rim of the cell, and then entry of a more robust population of fluor-molecules into the cell and then finally into the nucleus. Panels A, B, and C refer to control fluorescent-Tat peptide at 10 min, 1 h, and 2 h, respectively. The remaining panels (D, E, F) refer to the fluorescent **2-5A-tat** (compound **17**) at the same time points. The top 3 images of each panel are a higher magnification (2.5×) of the lower 3 images.

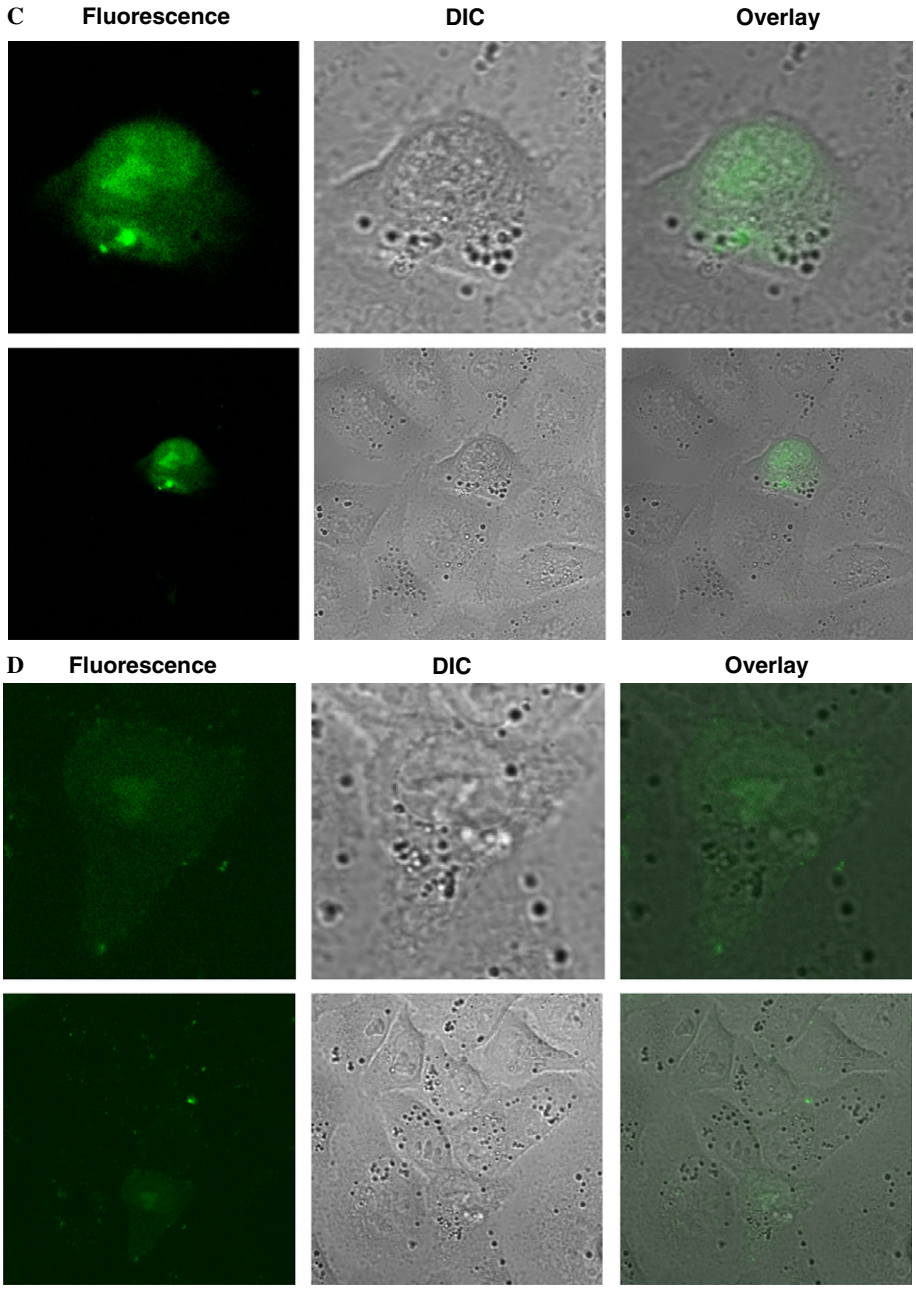

Figure 6. (*continued*)

ligation strategy employed 1,3-dipolar cycloaddition of a propargyl-cys-modified Tat peptide with a 2-5A derivative bearing a 2′-terminal aliphatic azido moiety. Both coupling reactions proceeded in good to excellent yields (60–80%).

In contrast to the problems of precipitation of aggregation seen in the preparation of other CPP-oligonucleotide conjugates, we observed no such issues with **2-5A-tat**, perhaps due to the much shorter electronegative oligonucleotide to which the electropositive Tat peptide was ligated.

Thus far, with but one exception, the synthetic approaches to CPP and Tat peptide-conjugated nucleic acids or nucleic acid analogues have been limited to ligation through formation of disulfide bonds.

When targeting P-glycoprotein or aberrant splicing in the Luciferase gene, Astriab-Fisher and co-workers conjugated Tat and Antennapedia peptides with oligodeoxyribonucleotide containing 5′-terminal 2-thiopyridyl groups.[5,31] A similar approach was employed by Allinquant et al.[32] in their generation of Attennapedia peptide coupled to antisense oligodeoxyribonucleotides against amyloid precursor protein and also by Troy et al.[33] for Attennapedia-coupled antisense oligonucleotides against Cu/Zn superoxide dismutase. Antopolsky et al.[34] ligated oligonucleotide phosphorothioates to the signal sequence of the

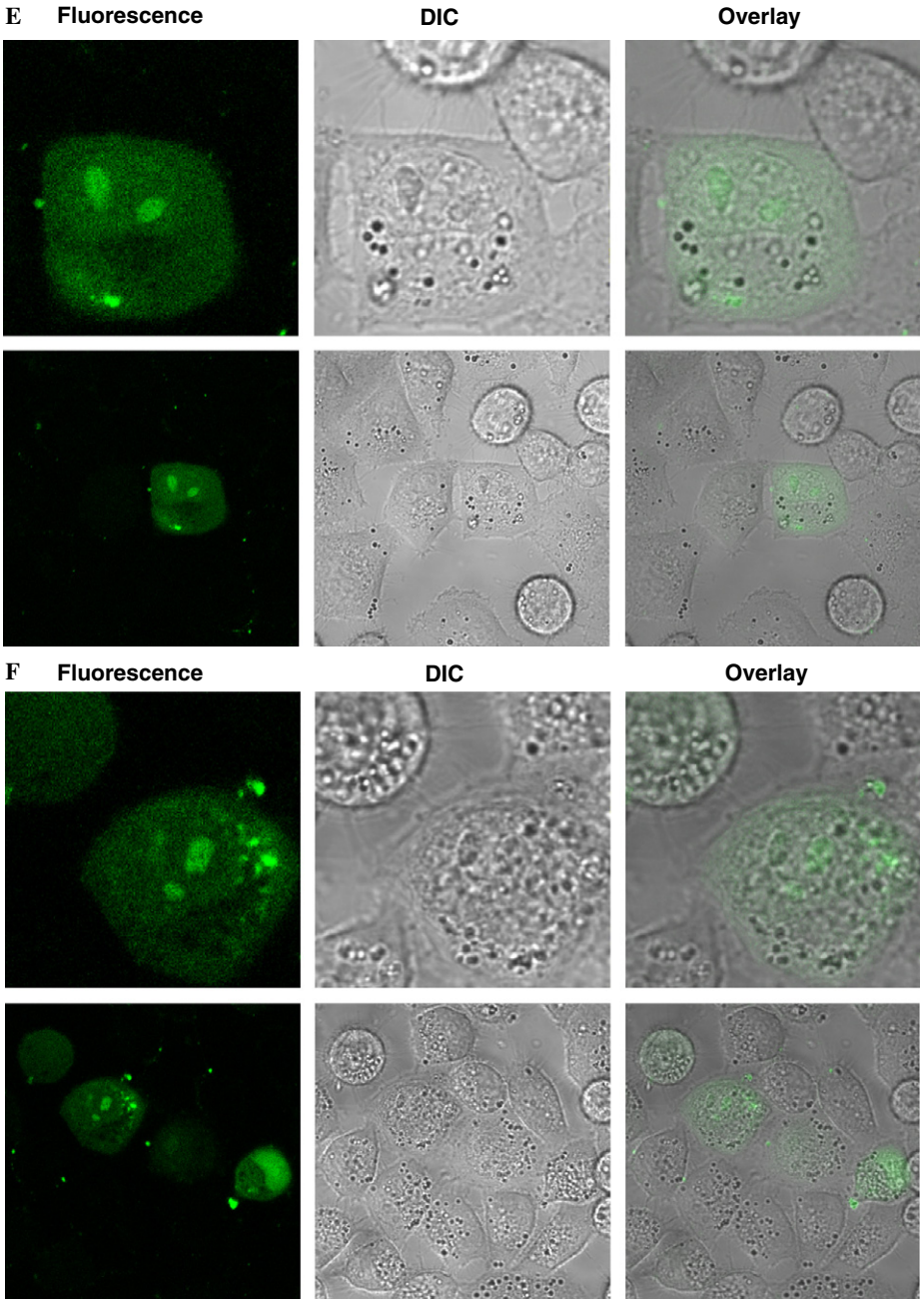

Figure 6. (*continued*)

Kaposi fibroblast growth factor by disulfide exchange with a mercaptoalkyl group tethered oligonucleotide phosphorothioate and a peptide containing a pyridyl disulfide functionality. Gait and co-workers[35] used the disulfide approach to prepare conjugates of copolymeric locked nucleic acids with 2′-O-methylated RNA with Tat peptide, transportan, penetratin, and related peptides. Prater and Miller[36] coupled 3′-methylphosphonate-terminated 2′-*O*-methyloligoribonucleotides to Tat peptide using a similar disulfide coupling strategy.

Maurel et al.[37] recently introduced a variation on the disulfide chemistry theme by generating a nitropyridyl disulfide functionalized oligonucleotide through the reaction of tritylthio-terminated oligonucleotide with a nitropyridylsulfenyl chloride.

The only exception to the use of disulfide chemistry in the pursuit of oligonucleotide-CPP conjugates arises from the efforts of Prater and Miller[36] who prepared a keto derivative of the Tat peptide by reacting a cysteine-terminated peptide with bromoacetone. This allowed oxime formation with the oligonucleotide that bore an introduced 5′-reactive amino embodied as 4-(2-aminooxyethoxy-2-(ethylureido)quinoline.

The hypothesis has forwarded (e.g., Maurel et al.[37]) that disulfide joined conjugates are advantageous because they are stable in cellular media, but would be severed

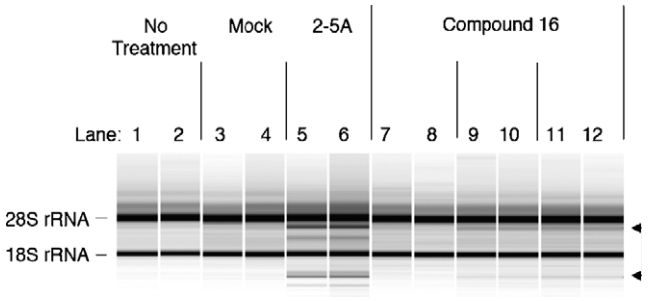

Figure 7. Compound **16** is able to enter cells unassisted and to activate intracellular RNase L. HeLa cells overexpressing RNase L were untreated, mock transfected with Fugene, transfected with trimer 2-5A using Fugene, or treated with compound **6** without uptake enhancer (as indicated in the figure). RNA was isolated and separated on an RNA Chip (Section 5). Positions of intact 28S and 18S rRNA (left) and specific rRNA cleavage products (arrow to the right of figure) are indicated. Lanes 1 and 2, untreated cells; lanes 3 and 4, mock treated cells; lanes 5 and 6, 2-5A (5 μM) plus Fugene; lanes 7 and 8, 125 nM **2-5A-tat**; lanes 9 and 10, 250 nM **2-5A-tat**; lanes 11 and 12, 500 nM **2-5A-tat**.

to component oligonucleotide and peptide in the reducing environment of the cells. From the perspective of the eventual hoped-for in vivo therapeutic application of nucleic acid- or nucleic acid analogue-CPP constructs, disulfide linkages will likely be counterproductive. Kwok et al.[38] studied the biodistribution, metabolic stability, and transient gene expression of sulfhydryl cross-linked peptide DNA formulations. They found that despite significant reductive stability of such disulfide-linked nucleic acid-peptides as measured in vitro, the intracellular reducing environment of the liver released DNA prematurely resulting in rapid metabolism. Thus, alternative more stable ligation chemistries, as developed herein, may be valuable additions to the bioconjugation schemes available for nucleic acid-CPPs, when eventual therapeutic endpoints are involved.

2-5A-tat conjugates were reduced significantly in RNase L activation ability as compared to the unligated 2-5A tetramer. These 30- to 100-fold reductions in RNase L activation ability, compared to unmodified 2-5A itself, are similar reductions in RNase L activation to that seen for chimeric 2-5A-antisense constructs of similar chain length. This comparison is valid when evaluation was carried out against RNA substrates that were non-complementary to the antisense domain of 2-5A-antisense analogues. Thus for instance, in the case of the 2-5A-antisense chimera with an all DNA phosphodiester DNA antisense domain that did not complement the substrate RNA, RNase L activation ability was reduced by about 30-fold compared to parent 2-5A.[29] When the antisense domain was a PNA[39] or morpholino analogue[40] that did not complement substrate RNA, then RNase L activation was reduced 60- to 100-fold. Greater activity has been observed when the antisense domain of the chimera targets specifically the RNA substrate. Thus, a 2-5A-antisense molecule with an all phosphodiester DNA targeting a specific sequence of PKR RNA was only three times less active than parent 2-5A.[41] This increase in activity against targeted substrate has been hypothesized to be related to a proximity effect due to creation of a new specific high-affinity binding site (the antisense domain of the 2-5A-antisense chimera) on RNase L.[41] In this case, it is clear from Figure 1 that **2-5A-tat** possesses similar RNase L activation competence to previously described molecules of this genre. As expected, AMP-S-tat and AMP-N-tat conjugates did not show the ability to activate RNase L (data not shown). This latter result is congruent with early reports that three intact adenine rings are needed for full RNase L binding ability.[1]

4. Conclusions

2-5A-tat conjugates provide a solution to one of chief roadblocks to the use of 2-5A as a therapeutic entity; namely, ineffective uptake of 2-5A itself. Historically, heroic and cell-unfriendly methods have been used to introduce 2-5A oligonucleotides into cells.[1] This has limited the experimental investigation of the biological effects of 2-5A as such methods are cumbersome, toxic to cells, and often of problematic reproducibility. The existence of a membrane-transportable version of 2-5A should permit a wider investigation of the biochemistry of 2-5A and RNase L. In addition, this conjugation approach might be extended to 2-5A-antisense itself to advance the potential of 2-5A-antisense as both a drug discovery target validation tool and as a potential therapeutic.

Another potential extension of this work applies to HIV therapeutics. While antiretroviral drugs effective against the HIV reverse transcriptase and protease enzymes represent milestones in the therapy of HIV infection, and have converted HIV infection into a chronic disease that requires lifelong therapy, highly active antiretroviral therapy (HAART),[42] once regarded by some as a potential cure for HIV infection, is limited by emerging problems[43–45] of HIV infection.[46] Such considerations make it imperative that new antiretroviral drugs be developed to provide less toxic treatments and to allow options for salvage therapy.[47,48] Ideally these agents should possess mechanisms of action that depart from the established reverse transcriptase and protease inhibitors. Indeed, promising options are being pursued including integrase inhibitors,[49,50] oligonucleotides,[51–53] fusion inhibitors,[54–58] and agents that interfere with HIV gene regulation.[59–64]

This research makes possible employment of a peptide as the targeting agent for 2-5A. Specifically, the constitutive, latent, and potent 2-5A-dependent RNase L could be targeted to the HIV RNA by the accomplished conjugating 2′,5′-oligoadenylates (2-5A) with Tat peptides to provide **2-5A-tat**. As with the previously demonstrated 2-5A-antisense strategy, this may result in the selective ablation of HIV RNA and inhibition of HIV replication. The Tat-derived peptide(s) domain of the **2-5A-tat** conjugate would bind to TAR of HIV RNA, and the appended 2-5A domain would attract and activate the 2-5A-dependent RNase L to this region of HIV RNA, resulting in its selective

cleavage by a catalytic mechanism. This possibility of selective inhibition of HIV replication is presently under active investigation.

5. Experimental

Except where otherwise noted, all reversed-phase HPLC analysis and purifications were conducted on a Varian Pro Star 210 instrument using Adsorbosphere ODS analytical (4.6×250 mm) and semi-preparative (10×250 mm) C-18 and C-8 columns (Alltech Company) for analysis and purification with the following buffers: (buffer A) 50 mM NH_4OAc (pH 7.00); (buffer B) 50% MeOH/H_2O. Linear gradient elution was employed with flow rate of 1 mL/min for analytic and 5 mL/min for preparative application. ^1H NMR (400.14 MHz), ^{31}P NMR (169.99 MHz), and ^{13}C NMR (100.62 MHz) spectra were recorded on Varian (Palo Alto, CA) VNMR 400 spectrometer. High resolution ESI mass spectrometry (HRESI) was recorded on an IonSpec Fourier Transform Mass Spectrometer at University of Arizona (Tucson, AZ). Matrix-assisted laser desorption/ionization time-of-flight mass spectrometry (MALDI-TOF/MS) was carried out on Kratos MALDI III instrument at HT laboratories (San Diego, CA). The chemical shifts are reported in parts per million (ppm) relative to internal tetramethylsilane in $CDCl_3$ or DMSO-d_6 (^1H NMR) or relative to H_3PO_4 (^{31}P NMR). The coupling constants (J) are reported in Hertz (Hz). UV spectra were determined on a Hewlett Packard 8452 spectrophotometer. The reagents 5′-AMP, $NaBH_3CN$, $CuSO_4$, $NaIO_4$, sodium ascorbate, and 6-heptynoic acid were purchased from Aldrich–Sigma (St Louis, MO). All amino acids and resin were purchased from Advanced Chemtech.

5.1. Peptide synthesis

Peptide **5** containing the translocation sequence of the tat peptide and alkyne functional group was synthesized using 0.25 mmol scale on a ABI 431 peptide synthesizer using standard FOMC chemistry with HOBt/HBTU/DIEA as activating reagents and using 20% piperidine for FMOC removal. The peptide sequence is 6-heptynoic-Gly-Gly-Arg-*Arg-Lys-Lys-Arg-Arg-Gln-Arg-Arg-Arg*-COOH (the italicized amino acids correspond to residues 48–57 RKKRRQRRR of the tat protein). The resin used was FMOC-Arg-Wang resin with 0.61 mmol/g loading. All arginines were double coupled and the alkyne moiety was coupled using 6-heptynoic acid. The peptide was cleaved with TFA/TIPS/water (93:5:2) for 5 h and purified by reversed-phase HPLC with an YMC-Pack ODS column (150×20 mm, Waters). MALDI-MS $(M+1)^+$: calcd for 1719.04; found: 1719.1.

Similar procedures were employed for the synthesis and purification of peptide **14** that contained two spacer glycine residues and then the terminal cysteine moiety. The product's structure was corroborated by ESI-MS. MS $(M+1)^+$: calcd for $C_{60}H_{118}N_{33}O_{14}S$: 1557; found: 1557.

5.2. Modification of AMP with azido functional group; synthesis of compound 3

Compound **3** was synthesized from 5′-AMP (**2**) and excess 3-azidopropanamine. Thus, sodium periodate solution (0.6 mL of 0.1 M in water, 60.0 μmol) was added in one portion to a solution of AMP (17.35 mg in 0.5 mL water, 50.0 μmol), and the resulting mixture was stirred in the dark at 0 °C for 30 min. To destroy the excess periodate, a $Na_2S_2O_3$ solution (1.0 mL of 0.1 M, 100.0 μmol) was added, and the resultant solution was maintained at 0 °C for an additional 10 min in the dark. 3-Azidopropanamine (25.0 mg, 250.0 μmol) was added, and the pH of the reaction mixture was adjusted to 8.6 with 5% acetic acid. The resulting mixture was stirred at 0 °C for 2 h and then a sodium cyanoborohydride solution (1 mL of 0.5 M in water, 0.5 mmol) was added. This reaction mixture was kept at 0 °C for 1 h during which time the pH was maintained at 6.6 by periodic addition of 0.5% HOAc. The reaction mixture was stirred at 4° overnight after which HPLC analysis showed the reaction was complete. The product **3** was purified by HPLC on semi-preparative Adsorbosphere C-18 column (10×250 mm) (82% yield) and its structure corroborated by ^1H NMR, ^{13}P NMR, and high resolution mass spectroscopy (HRMS). ^1H NMR (CD_3OD) δ (ppm) 1.85 (m, 2 H, $-CH_2-$); 2.37 (t, $J = 10.8$ Hz, 1H, H-3′); 2.71 (t, $J = 7.2$ Hz, 2H, $-CH_2N$), 2.81 (m, 1H, H-2′); 3.15–3.31 (m, 2H, H-2′, H-3′); 3.40 (t, $J = 7.2$ Hz, 2H, $-CH_2N_3$); 3.99 (m, 2H, H-5′, H-5′); 4.20 (m, 1H, H-4′); 6.00 (dd, $J = 10.0$, 2.4 Hz, 1H, H-1′); 8.19 (s, 1H); 8.25 (s, 1H). ^{31}P NMR (CD_3OD) δ (ppm) 1.94. HRESI MS calcd for $C_{13}H_{20}N_9O_5P$: 414.1403 $(M+1)^+$; found: 414.1391.

5.3. Coupling between 2-5A tetramer and 3-azidopropanylamine: synthesis of compound 4

A solution of $NaIO_4$ (0.1 M 4.0 μL, 0.4 μmol) was added to a cooled solution of p5′A2′p5′A2′p5′A2′p5′A (80 μL, 8.8 OD, 0.2 μmol). The oxidation was carried out at 0 °C in the dark for 90 min. Then a 2-fold excess of $Na_2S_2O_3$ over $NaIO_4$ was added to the solution to remove the excess oxidant. The reaction mixture was stirred for another 10 min. After that, 3-azidopropanylamine (16.0 μL of 0.05 M, 0.8 μmol) was added, and the pH was adjusted to 8.6 with 0.5% HOAc. After 3.5 h, 4.0 μL of 0.5 M $NaBH_3CN$ was added, and the pH was adjusted to about 6.6. After overnight incubation, the product was purified by HPLC to afford **4** in 45% yield. The product **4** was analyzed by MALDI-TOFF mass spectrometry: calcd for $C_{43}H_{56}N_{24}O_{23}P_4$: 1400.9; found: 1401).

5.4. Conjugation products from azide-alkyne cycloaddition: synthesis of compounds 6 and 7

Compound **3** (0.8 mg, 2 μmol) and tat peptide **5** (1.7 mg, 1 μmol) were dissolved in water (30 μL). Sodium ascorbate (1 μmol, 1 μL of freshly prepared 1 M solution in water) was added, followed by copper(II) sulfate solution (1 μmol, 10 μL of 0.1 M in water). The mixture was stirred vigorously for 24 h. The reaction mixture

was purified by a DEAE Sephadex column and the eluted fraction was lyophilized to give the product **6** (9.2 OD, 60%). The product was analyzed by MALDI-TOFF mass spectrometry: calcd for $C_{83}H_{152}N_{45}O_{20}P$: 2131; found: 2131).

The reaction between the azido-functionalized 2-5A tetramer **4** and tat peptide **5** was carried out under similar reaction conditions with a similar purification protocol The product's structure was corroborated by MALDI-TOFF mass spectrometry: calcd for $C_{113}H_{188}N_{60}O_{38}P_4$: 3118; found: 3118.

5.5. Synthesis of *p*-(*N*-chloroacetamido)benzylamine (compound 11)

Chloroacetyl chloride (**9**, 0.64 mL, 8.0 mmol) in 5 mL dry THF was added dropwise into a mixture of sodium bicarbonate (1.0 g, 10.0 mmol), 4-[(*N*-Boc)aminomethyl]aniline (**8**, 473 mg, 97%, 2 mmol), and dry THF (15 mL) at 0 °C (ice-bath) under N_2 atmosphere over a period of 10 min. The resultant mixture was stirred for another 2 h as the temperature was allowed to rise from 0 °C to room temperature. The reaction mixture was then poured into a sodium bicarbonate solution, and extracted with ethyl acetate (3× 50 mL). The combined organic solvent was dried over sodium sulfate and then evaporated to produce a white powder **10** (quantitative yield). ^{1}H NMR ($CDCl_3$) δ (ppm) 1.45 (s, 9H, CH_3); 4.18 (s, 2H, CH_2); 4.28 (s, 2H, CH_2); 4.84 (s, 1H, NH); 7.25–7.28 (dd, 4H, ArH); 8.23 (s, 1H, NH). ^{13}C NMR ($CDCl_3$) δ (ppm) 28.3, 42.8, 44.1, 79.5, 120.3, 128.2, 135.8, 135.9, 155.8, 163.7.

Next a hydrogen chloride solution in dioxane (2.5 mL, 4 M) was added into a suspension of compound **10** and dry ethyl acetate (2.5 mL) at 0 °C. The mixture was allowed to stir for 2 h at ice temperature. After removal of the organic solvent under reduced pressure, a white solid product **11** was obtained (200 mg, 85% yield). ^{1}H NMR (D_2O δ (ppm) 4.06 (s, 2H, CH_2); 4.17 (s, 2H, CH_2); 7.34–7.42 (m, 4H, ArH). ^{13}C NMR (D_2O) δ (ppm) 42.8, 43.0, 122.6, 129.9, 130.2, 137.1, 168.5.

5.6. Synthesis of compound 12 from AMP and *p*-[*N*-(α-chloroacetamido)]benzylamine (11)

Sodium periodate solution (0.6 mL 0.1 M in water, 60.0 μmol) was added in one portion to a solution of AMP (17.35 mg in 0.5 mL water, 50.0 μmol), and the resulting mixture was stirred in the dark at 0 °C for 30 min. To destroy the excess periodate, a $Na_2S_2O_3$ solution (1.0 mL of 0.1 M, 100 μmol) was added, and the resultant solution was maintained at 0 °C for an additional 10 min in the dark. An aqueous solution of compound **11** (1 mL, 23.5 mg, 100.0 μmol) was added, and the pH of the reaction mixture was adjusted to 8.6 with 2 N NaOH. The resulting mixture was stirred at 0 °C for 2.5 h and then a sodium cyanoborohydride solution (0.5 mL of 0.5 M in water, 0.25 mmol) was added. This mixture was kept at 0 °C for 1 h during which time the pH was maintained at 6.3 by periodic addition of 0.5% HOAc. After the reaction mixture was stirred at 4 °C overnight, HPLC analysis showed the reaction was complete. The product **12** was purified by HPLC on semi-preparative Adsorbosphere C-18 column (10× 250 mm) (85% yield) and its structure corroborated by ^{1}H NMR, ^{13}P NMR, and mass spectroscopy (MS). ^{1}H NMR (D_2O) δ (ppm) 2.28 (t, J = 12.0 Hz, 1H, H-3′); 2.67 (t, J = 10.4 Hz, 1H, H-2′); 2.90–2.99 (m, 2H, H-2′, H-3′); 3.52–3.70 (m, 2H, H-5′, H-5′); 3.78 (s, 2H, CH_2); 4.06 (m, 1H, H-4′); 4.11 (s, 2H, CH_2); 5.72 (d, J = 9.6, Hz, 1H, H-1′); 7.20–7.28 (m, 4H, ArH); 8.03 (s, 1H); 8.07 (s, 1H). ^{13}C NMR (D_2O) δ (ppm) 43.5, 53.7, 55.1, 61.0, 64.4, 75.2, 79.0, 118.4, 119.2, 129.4, 132.6, 137.5, 138.9, 148.8, 152.7, 155.9, 164.4; ^{31}P NMR (D_2O) δ (ppm) 2.01. ESI MS calcd for $(M+1)^+$ $C_{19}H_{23}ClN_7O_6P$: 512; found: 512.

5.7. Synthesis of compound 13

$NaIO_4$ solution (0.1 M, 4.0 μL, 0.4 μmol) was added to a cooled solution of 2-5A tetramer (**1**) (80 μL, 8.8 OD, 0.2 μmol), and the oxidation was allowed to proceed at 0 °C in the dark for 90 min. Then a twofold excess of $Na_2S_2O_3$ over $NaIO_4$ was added to the solution to remove the excess oxidant. The reaction mixture was stirred for another 10 min. After that, compound **11** (20.0 μL of 0.1 M, 2.0 μmol) was added, and the pH was adjusted to about 8.4 with 0.1 M NaOH. After the mixture had been stirred at 0 °C for 2.5 h, 4.0 μL of 0.5 M $NaBH_3CN$ was added, and the pH was adjusted to 6.4 with 0.5% HOAc. After overnight incubation, the product was purified by HPLC to afford compound**13**. The product was analyzed by HRMS mass spectrometry: calcd for $C_{49}H_{60}ClN_{22}O_{24}P_4$: 1499.279; found: 1499.4439).

5.8. Synthesis of Tat peptide conjugation products, compounds 15 and 16

Peptide **14** and compound **12** (3 mg, 5.8 μmol) were dissolved in acetonitrile (50 μL). Then buffer (200 μL of 0.1 M NaH_2PO_4) was added into the mixture under a nitrogen atmosphere. After the mixture was stirred at room temperature for 4 h under N_2, the product was separated using a DEAE Sephadex A-25 column with acetonitrile/water (50:50) solution as eluent. The collected fractions were lyophilized to give the product **15** (6.4 OD, 73% yield). The product was analyzed by ESI mass spectrometry: calcd for $C_{79}H_{139}N_{40}O_{20}PS$: 2032; found: 2032).

The reaction between the chloroacetyl-functionalized 2-5A tetramer **13** and tat peptide **14** was carried out under similar reaction conditions. The product's structure was corroborated by MALDI-TOF mass spectrometry: calcd for $C_{109}H_{175}N_{55}O_{38}P_4S$: 3019; found: 3017).

5.9. Synthesis of 2-5A-S-Tat-fluorescein (compound 17)

Acetonitrile (50 μL) was added to a mixture of the chloroacetamido derivative (**13**, 0.27 μmol) of 2-5A and the cysteine-terminated tat peptide labeled with fluorescein (0.09 μmol). Then buffer (200 μL, 0.1 M NaH_2PO_4)

was added to the above mixture under a nitrogen atmosphere. The mixture was stirred at room temperature for 24 h under N_2, and the product was separated using a DEAE–Sephadex A-25 column with CH_3CN/H_2O (50:50) as eluent. The collected fraction was lyophilized to give the product 2-5A-S-Tat-fluorescein (1.2 OD, 30% yield). The conjugate product was confirmed by MALDI-TOFF mass spectrometry: calcd for $C_{132}H_{188}N_{56}O_{45}P_4S$: 3435; found: 3435).

5.10. RNase L assay

RNase L activity was determined by a fluorescence resonance energy transfer (FRET) method (*35, Thakur 2005*). The assay uses recombinant human RNase L produced in insect cells from a baculovirus vector and purified by FPLC columns (36). The cleavable substrate consists of a 36 nucleotide synthetic oligoribonucleotide sequence derived from respiratory syncytial virus with the fluorophore, FAM, at the 5′-terminus and black hole quencher-1 (BHQ-1), at the 3′-terminus (synthesized at Integrated DNA Technologies). The RNA sequence contains several cleavage sites for RNase L (UU or UA). The test compounds or 2-5A were diluted to final concentrations of 1, 3, 10, 30, 100, 300, 1000, and 3000 nM in DEPC-treated water. Five microliters of each diluted sample was added in triplicate to 96-well black polystyrene microtiter plates (Corning) on ice. Forty-five microliters of the reaction mixture was added to each sample and the plates were gently agitated for 10 s to mix, then were centrifuged briefly at 500 rpm. The assays contained 100 nM RNA probe, 25 nM RNase L, 25 mM Tris–HCl (pH 7.4), 100 mM KCl, 10 mM $MgCl_2$, 50 μM ATP, and 7 mM 2-mercaptoethanol with and without 2-5A or other compounds. RNase L was the last component added to the reaction mixtures. The plates were incubated at 20 °C protected from light. Fluorescence was measured at 5, 30, 60, 90, and 120 min with a Wallac 1420 fluorimeter (Perkin Elmer) (absorption 485 nm/emission 535 nm).

5.11. Activation of RNase L in intact cells

RNase L activity assays were performed in intact cells. HeLa M cells expressing wild-type human RNase L cDNA in plasmid pcDNAneo3 (Invitrogen, San Diego, CA) (J.M.P. and R.H.S., to be described elsewhere) were grown in DMEM supplemented with streptomycin/penicillin, 300 mg/ml geneticin (Invitrogen), and 10% heat-inactivated fetal bovine serum. Transfection of 2-5A trimer was performed using Fugene 6 (Roche Diagnostic) according to the manufacturer's protocol. Briefly, cells were plated a day prior to transfection to give ~75–80% confluency at the time of transfection. 2-5A trimer (p3A3) was diluted into OptiMEM™ media (Invitrogen) and then mixed with Fugene 6 for 30 min. The mixture was added to the cells, incubated at 37 °C for 6 h, and then media were removed and cells were washed twice with PBS, RNA was isolated with Trizol reagent (Invitrogen). Separately, HeLa cells were treated with compound **16** at the concentration indicated in the legend to Figure 6. Protamine (0.01%) (Cat. P4005, Sigma) was added to cells in DMEM containing 2% FBS prior to treatment. The pipette tip was dipped in serum prior to pipetting compound **16** to avoid attachment to plastic tip. Compound **16** was diluted with complete medium plus 2% FBS prior to adding to cells. After 6 h incubation with compound **16** at 37 °C, media were removed and cells were washed twice with PBS. Isolated RNA (1 μg) was separated on RNA chips (Agilent Technologies) and analyzed with an Agilent Bioanalyzer 2100 (Agilent Technologies).

5.12. Uptake of Tat

HeLa cells were cultured in 200 μl DMEM (Cambrex), supplemented with 10% fetal bovine serum (FBS) (HyClone), glutamine, penicillin/streptomycin (Gemini Bio Products), and 0.01% protamine (Sigma P4005). Fluorescently labeled **2-5A-tat** peptide conjugate (**2-5A-tat**) and fluorescent-tat-SH were added to cells to a final concentration of 1 μM. Before adding the peptides to the cells, pipette-tips were dipped in serum; tat-peptides will otherwise stick to the plastic tips. After 10 min, one hour, and two hours, the medium was replaced with PBS (Cambrex). Images of cellular uptake of our compounds were acquired with a Zeiss LSM410 laser scanning confocal microscope equipped with a mixed-gas laser (488-, 568-, and 647-nm excitation lines) in sequential scans then analyzed with Microcosm Renaissance 410 software. Overlays of the acquired images were generated using Adobe Photoshop CS software.

Acknowledgments

PFT thanks the National Institute of Allergy and Infectious Diseases for support from Grant 5 R03 AI054184-02, Robert Smith for excellent technical assistance, and Edgar Civitello for advice in peptide synthesis.

References and notes

1. Player, M. R.; Torrence, P. F. *Pharmacol. Ther.* **1998**, *78*, 55–113.
2. Sen, G. C. *Annu. Rev. Microbiol.* **2001**, *55*, 255–281.
3. Weeks, K. M.; Ampe, C.; Schultz, S. C.; Steitz, T. A.; Crothers, D. M. *Science* **1990**, *249*, 1281–1285.
4. Vives, E. *J. Control. Release* **2005**, *109*, 77–85.
5. Astriab-Fisher, A.; Sergueev, D.; Fisher, M.; Shaw, B. R.; Juliano, R. L. *Pharm. Res.* **2002**, *19*, 744–754.
6. Gatignol, A.; Jeang, K. T. *Adv. Pharmacol.* **2000**, *48*, 209–227.
7. Gelus, N.; Bailly, C.; Hamy, F.; Klimkait, T.; Wilson, W. D.; Boykin, D. W. *Bioorg. Med. Chem.* **1999**, *7*, 1089–1096.
8. Gelus, N.; Hamy, F.; Bailly, C. *Bioorg. Med. Chem.* **1999**, *7*, 1075–1079.
9. Hamy, F.; Brondani, V.; Florsheimer, A.; Stark, W.; Blommers, M. J.; Klimkait, T. *Biochemistry* **1998**, *37*, 5086–5095.
10. Hamy, F.; Gelus, N.; Zeller, M.; Lazdins, J. L.; Bailly, C.; Klimkait, T. *Chem. Biol.* **2000**, *7*, 669–676.
11. Huq, I.; Ping, Y. H.; Tamilarasu, N.; Rana, T. M. *Biochemistry* **1999**, *38*, 5172–5177.

12. Hwang, S.; Tamilarasu, N.; Ryan, K.; Huq, I.; Richter, S.; Still, W. C.; Rana, T. M. *Proc. Natl. Acad. Sci. U.S.A.* **1999**, *96*, 12997–13002.
13. Hwu, J. R.; Tseng, W. N.; Gnabre, J.; Giza, P.; Huang, R. C. *J. Med. Chem.* **1998**, *41*, 2994–3000.
14. Jackson, W. H., Jr.; Moscoso, H.; Nechtman, J. F.; Galileo, D. S.; Garver, F. A.; Lanclos, K. D. *Biochem. Biophys. Res. Commun.* **1998**, *245*, 81–84.
15. Klimkait, T.; Felder, E. R.; Albrecht, G.; Hamy, F. *Biotechnol. Bioeng.* **1998**, *61*, 155–168.
16. Mayhood, T.; Kaushik, N.; Pandey, P. K.; Kashanchi, F.; Deng, L.; Pandey, V. N. *Biochemistry* **2000**, *39*, 11532–11539.
17. Mei, H. Y.; Cui, M.; Heldsinger, A.; Lemrow, S. M.; Loo, J. A.; Sannes-Lowery, K. A.; Sharmeen, L.; Czarnik, A. W. *Biochemistry* **1998**, *37*, 14204–14212.
18. Michaelis, K.; Kalesse, M. *Angew. Chem. Int. Ed. Engl.* **1999**, *38*, 2243–2245.
19. Tamilarasu, N.; Huq, I.; Rana, T. M. *Bioorg. Med. Chem. Lett.* **2000**, *10*, 971–974.
20. Tamilarasu, N.; Huq, I.; Rana, T. M. *Bioorg. Med. Chem. Lett.* **2001**, *11*, 505–507.
21. Tok, J. B.; Des Jean, R. C.; Fenker, J. *Bioorg. Med. Chem. Lett.* **2001**, *11*, 43–46.
22. Harju, K.; Yli-Kauhaluoma, J. *Mol. Divers* **2005**, *9*, 187–207.
23. Kotha, S.; Lahiri, K. *Curr. Med. Chem.* **2005**, *12*, 849–875.
24. Demko, Z. P.; Sharpless, K. B. *Org. Lett.* **2001**, *3*, 4091–4094.
25. Himo, F.; Demko, Z. P.; Noodleman, L.; Sharpless, K. B. *J. Am. Chem. Soc.* **2002**, *124*, 12210–12216.
26. Rostovtsev, V. V.; Green, L. G.; Fokin, V. V.; Sharpless, K. B. *Angew. Chem. Int. Ed. Engl.* **2002**, *41*, 2596–2599.
27. Wang, Q.; Chan, T. R.; Hilgraf, R.; Fokin, V. V.; Sharpless, K. B.; Finn, M. G. *J. Am. Chem. Soc.* **2003**, *125*, 3192–3193.
28. Thakur, C. S.; Xu, Z.; Wang, Z.; Novince, Z.; Silverman, R. H. *Methods Mol. Med.* **2005**, *116*, 103–113.
29. Dong, B.; Xu, L.; Zhou, A.; Hassel, B. A.; Lee, X.; Torrence, P. F.; Silverman, R. H. *J. Biol. Chem.* **1994**, *269*, 14153–14158.
30. Wreschner, D. H.; James, T. C.; Silverman, R. H.; Kerr, I. M. *Nucleic Acids Res.* **1981**, *9*, 1571–1581.
31. Astriab-Fisher, A.; Sergueev, D. S.; Fisher, M.; Shaw, B. R.; Juliano, R. L. *Biochem. Pharmacol.* **2000**, *60*, 83–90.
32. Allinquant, B.; Hantraye, P.; Mailleux, P.; Moya, K.; Bouillot, C.; Prochiantz, A. *J. Cell Biol.* **1995**, *128*, 919–927.
33. Troy, C. M.; Derossi, D.; Prochiantz, A.; Greene, L. A.; Shelanski, M. L. *J. Neurosci.* **1996**, *16*, 253–261.
34. Antopolsky, M.; Azhayeva, E.; Tengvall, U.; Auriola, S.; Jaaskelainen, I.; Ronkko, S.; Honkakoski, P.; Urtti, A.; Lonnberg, H.; Azhayev, A. *Bioconjug. Chem.* **1999**, *10*, 598–606.
35. Turner, J. J.; Arzumanov, A. A.; Gait, M. J. *Nucleic Acids Res.* **2005**, *33*, 27–42.
36. Prater, C. E.; Miller, P. S. *Bioconjug. Chem.* **2004**, *15*, 498–507.
37. Maurel, F.; Debart, F.; Cavelier, F.; Thierry, A. R.; Lebleu, B.; Vasseur, J. J.; Vives, E. *Bioorg. Med. Chem. Lett.* **2005**, *15*, 5084–5087.
38. Kwok, K. Y.; Park, Y.; Yang, Y.; McKenzie, D. L.; Liu, Y.; Rice, K. G. *J. Pharm. Sci.* **2003**, *92*, 1174–1185.
39. Verheijen, J. C.; van der Marel, G. A.; van Boom, J. H.; Bayly, S. F.; Player, M. R.; Torrence, P. F. *Bioorg. Med. Chem.* **1999**, *7*, 449–455.
40. Zhou, L.; Civitello, E. R.; Gupta, N.; Silverman, R. H.; Molinaro, R. J.; Anderson, D. E.; Torrence, P. F. *Bioconjug. Chem.* **2005**, *16*, 383–390.
41. Maitra, R. K.; Li, G.; Xiao, W.; Dong, B.; Torrence, P. F.; Silverman, R. H. *J. Biol. Chem.* **1995**, *270*, 15071–15075.
42. Barbaro, G.; Scozzafava, A.; Mastrolorenzo, A.; Supuran, C. T. *Curr. Pharm. Des.* **2005**, *11*, 1805–1843.
43. Pereira, C. F.; Paridaen, J. T. *Curr. Pharm. Des.* **2004**, *10*, 4005–4037.
44. Turpin, J. A. *Expert Rev. Anti Infect. Ther.* **2003**, *1*, 97–128.
45. Daugas, E.; Rougier, J. P.; Hill, G. *Kidney Int.* **2005**, *67*, 393–403.
46. Lori, F.; Lisziewicz, J. *JAMA* **2001**, *286*, 2981–2987.
47. Miller, M. D.; Hazuda, D. J. *Curr. Opin. Microbiol.* **2001**, *4*, 535–539.
48. Smith, K. A. *Curr. Opin. Immunol.* **2001**, *13*, 617–624.
49. Pommier, Y.; Johnson, A. A.; Marchand, C. *Nat. Rev. Drug Discov.* **2005**, *4*, 236–248.
50. Van Maele, B.; Debyser, Z. *AIDS Rev.* **2005**, *7*, 26–43.
51. Becker, Y. *Virus Genes* **2005**, *30*, 251–266.
52. Nimjee, S. M.; Rusconi, C. P.; Sullenger, B. A. *Annu. Rev. Med.* **2005**, *56*, 555–583.
53. Phillips, M. I. *Methods Mol. Med.* **2005**, *106*, 3–10.
54. Wang, H. G.; Williams, R. E.; Lin, P. F. *Curr. Pharm. Des.* **2004**, *10*, 1785–1793.
55. Covington, L. W. *Nurs. Clin. North Am.* **2005**, *40*, 149–165.
56. Magden, J.; Kaariainen, L.; Ahola, T. *Appl. Microbiol. Biotechnol.* **2005**, *66*, 612–621.
57. Oldfield, V.; Keating, G. M.; Plosker, G. *Drugs* **2005**, *65*, 1139–1160.
58. Shaheen, F.; Collman, R. G. *Curr. Opin. Infect Dis.* **2004**, *17*, 7–16.
59. Andersen, J. L.; Planelles, V. *Curr. HIV Res.* **2005**, *3*, 43–51.
60. Bannwarth, S.; Gatignol, A. *Curr. HIV Res.* **2005**, *3*, 61–71.
61. Gibellini, D.; Vitone, F.; Schiavone, P.; Re, M. C. *New Microbiol.* **2005**, *28*, 95–109.
62. Joseph, A. M.; Kumar, M.; Mitra, D. *Curr. HIV Res.* **2005**, *3*, 87–94.
63. Zhao, R. Y.; Bukrinsky, M.; Elder, R. T. *Indian J. Med. Res.* **2005**, *121*, 270–286.
64. De Clercq, E. *J. Med. Chem.* **2005**, *48*, 1297–1313.